Seeing is believing - How to access the nanoworld

STM: Scanning Tunneling Microscope

Idea

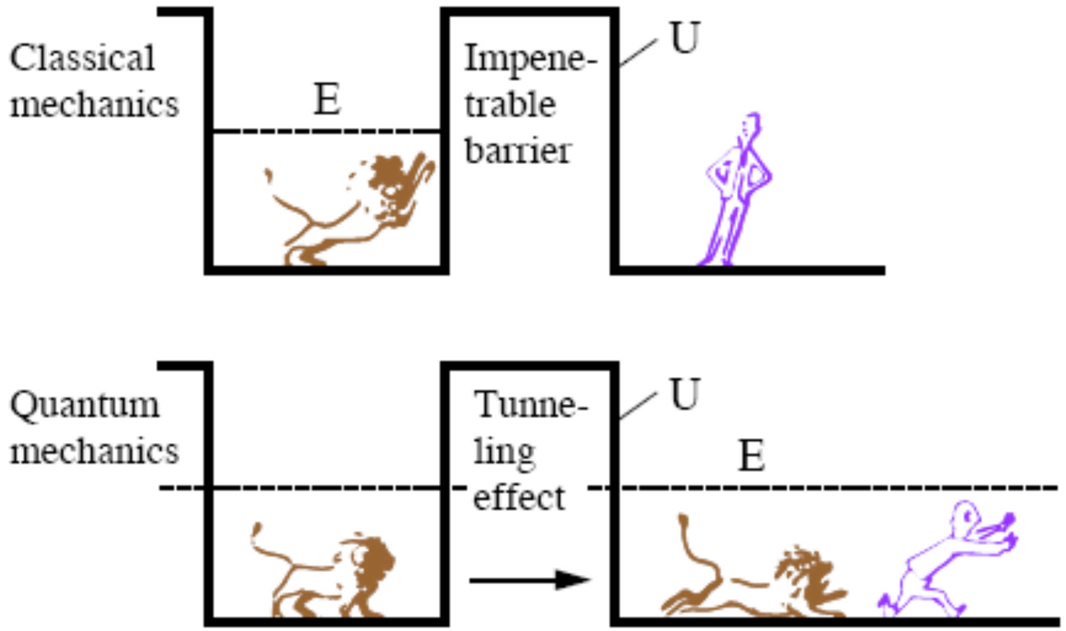

The difference between classical theory and quantum theory. In quantum mechanics, an electron has a nonzero probability of tunneling through a potential barrier. (After Van Vleck; see Walmsley, 1987.)

Working principle

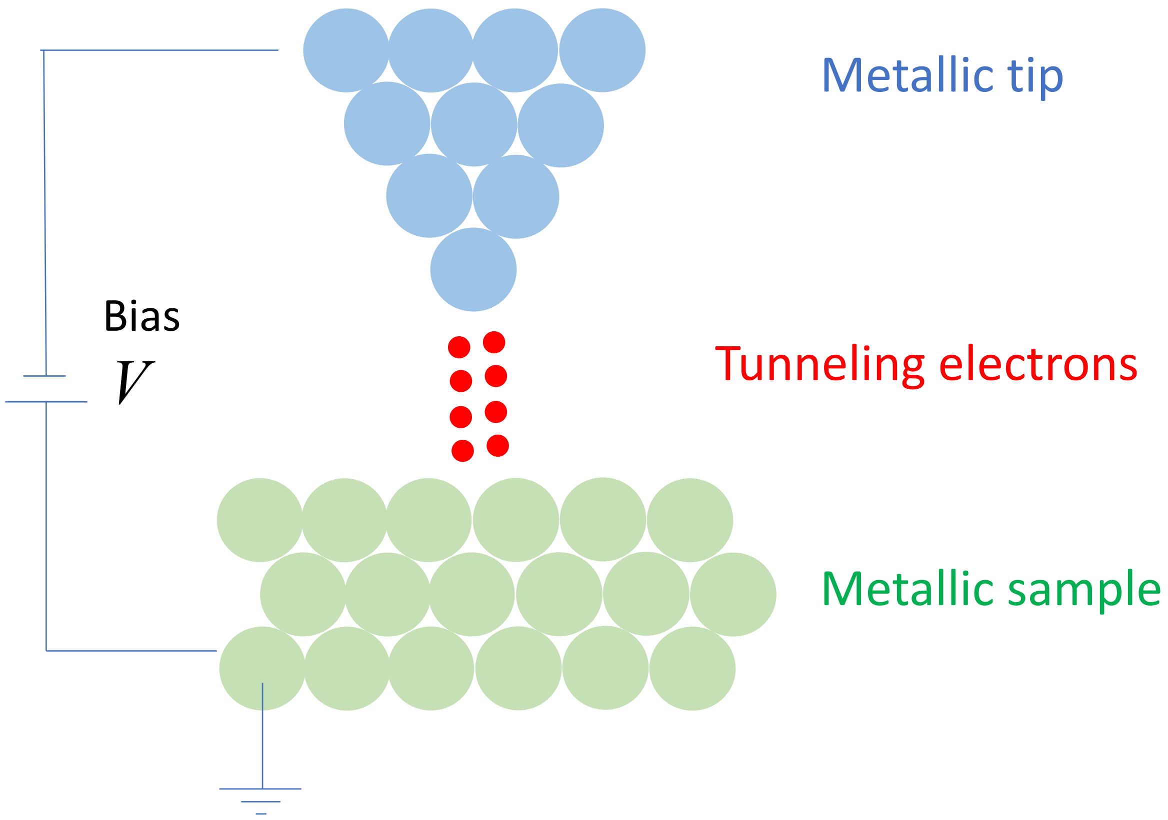

Quantum tunneling – 1D

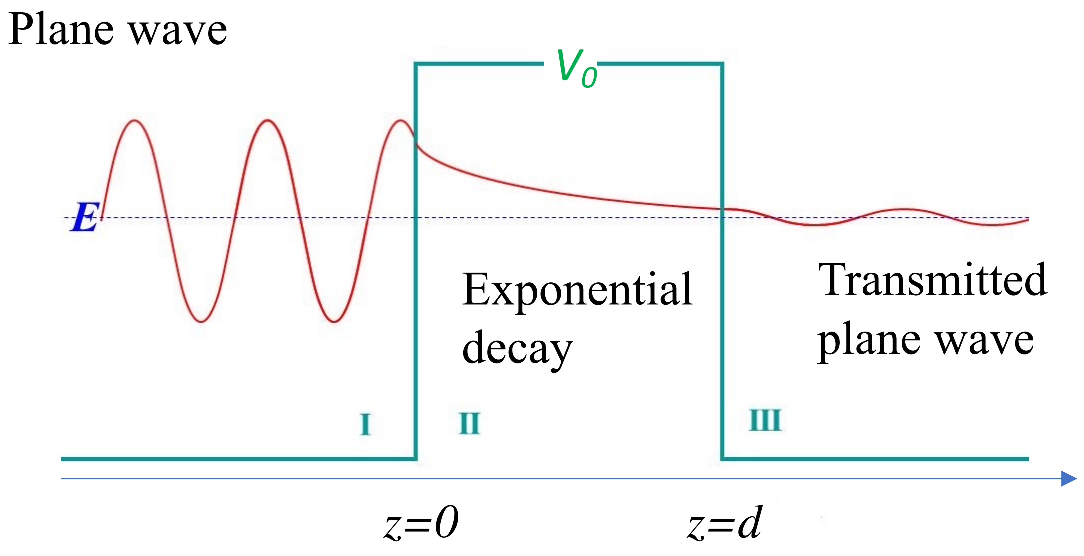

in region II (classically forbiden), exponential decay:

$$\psi(z) = \psi(0)e^{-\kappa z}$$

with $\kappa = \dfrac{\sqrt{2m(V_0 - E)}}{\hbar}$

in particular $\psi(d) = \psi(0)e^{-\kappa d}$

→ tunneling probability $\propto |\psi(d)|^2 = |\psi(0)|^2 e^{-2\kappa d}$

Quantum tunneling in a STM junction – 1D

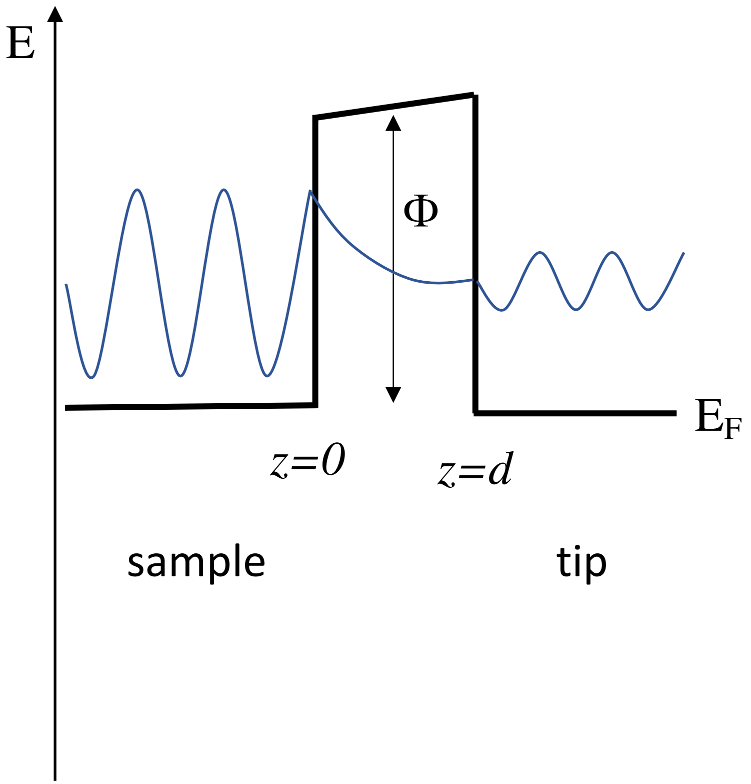

Tip and sample are very close to each other (distance d)
→ the Fermi levels of sample and tip align

We assume for simplicity that sample and tip have the same work function Φ, or we take the average value, to describe the barrier heigth

Typical work function of metals is 4-5 eV

with Φ= 4 eV → $\kappa = \frac{\sqrt{2m\,\Phi}}{\hbar} = 0.51\sqrt{\Phi(\mathrm{eV})}$ Å^{-1} ~ 1 Å^{-1}

$$|\psi(d)|^2 = |\psi(0)|^2 e^{-2\kappa d}$$

Δz =1 Å → $\exp(-2\kappa\Delta z) = \exp(-2) \sim 0.13$

For electrons at the Fermi level E_F of sample or tip, a variation in distance of 1 Å results in one order of magnitude difference in the tunneling probability

Tunneling current

J. Bardeen, Phys. Rev. Lett. **6**, 57 (1961).

Tip and sample described by two infinite planar electrodes.
Perturbative approach: start with “free” subsystems, eigenfunctions and respective energy levels

$\psi_{s,\mu}$ E_μ $\psi_{t,\nu}$ E_ν

The transition probability per unit time $w_{\mu\nu}$ of an electron from the sample state $\psi_{s,\mu}$ to the tip state $\psi_{t,\nu}$ is given by the Fermi golden rule:

$$w_{\mu\nu} = \frac{2\pi}{\hbar} \left| M_{\mu\nu} \right|^2 \delta\left(E_\mu - E_\nu\right)$$

δ → elastic tunneling (energy conservation)

The tunneling matrix element is determined by a surface integral on a surface between the two electrodes, giving the current density probability:

$$M_{\mu\nu} = \frac{\hbar^2}{2m} \iint \left(\psi_{t,\nu}^* \frac{d\psi_{s,\mu}}{dz} - \psi_{s,\mu} \frac{d\psi_{t,\nu}^*}{dz} \right) dx\, dy$$

So far: tunneling form a single state μ to a single state ν. However tip and substrate are characterized by many electronic states, thus we have to consider the sum of $w_{\mu\nu}$ over all states μ and ν.

In addition we can go from discrete levels to the density of states : $\sum_{\mu\nu} \rightarrow \int \rho_s\, \rho_t$

Tunneling current

If there is no bias applied, there is no net current across the junction.

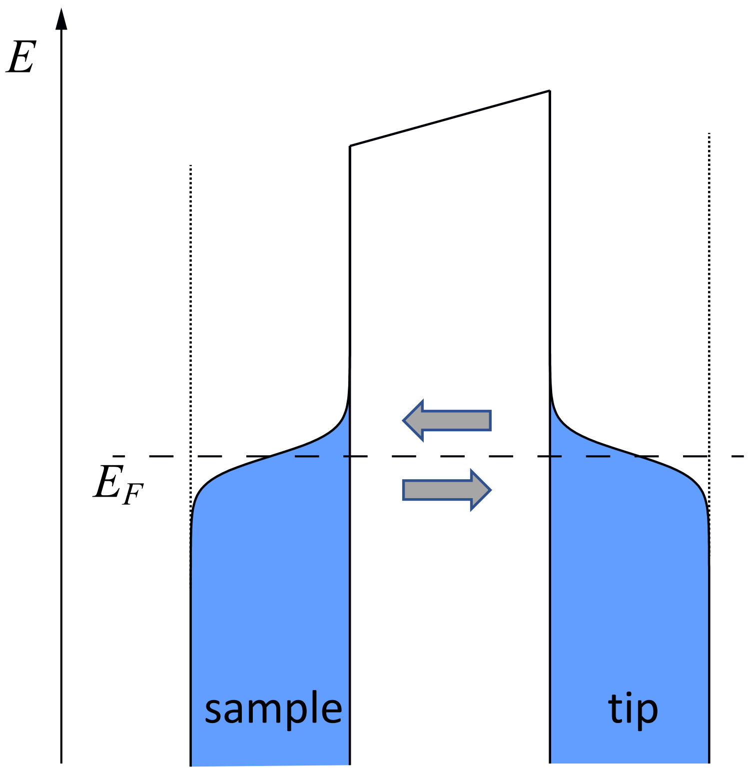

By applying a bias voltage V, a net tunneling current appears.

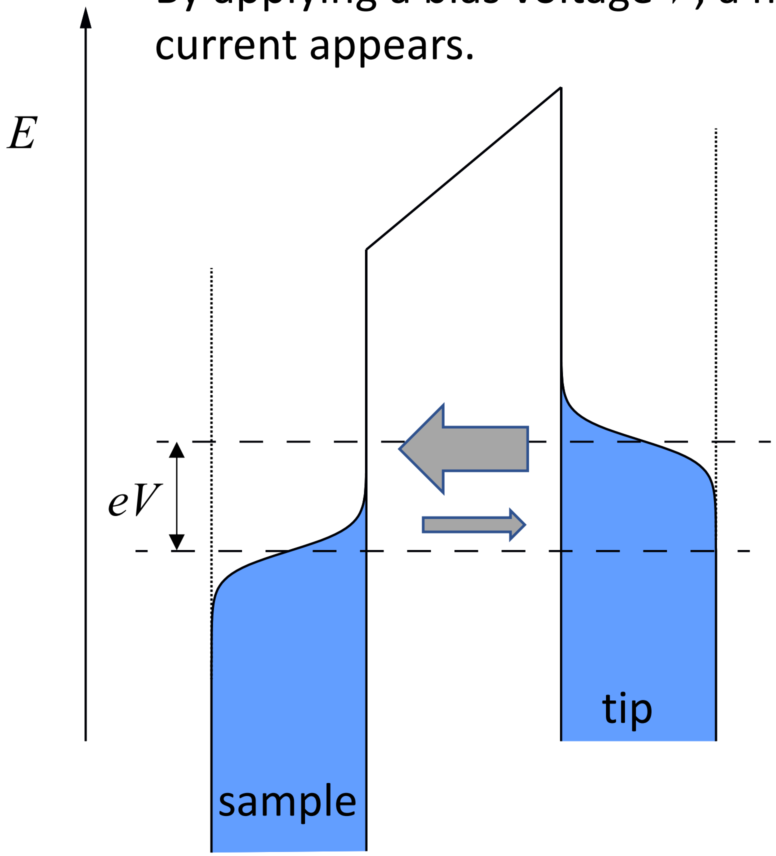

Fermi function

$$f(E,T) = \frac{1}{\exp\left(\frac{E-E_F}{k_B T}\right)+1}$$

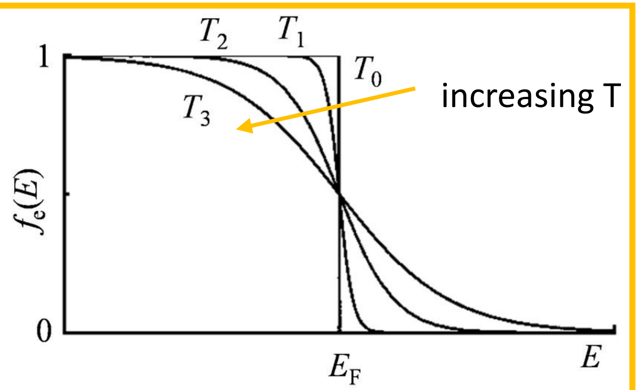

Tunneling current

$$I_{t\to s} = \frac{4\pi e}{\hbar}\int_{-\infty}^{+\infty} \underbrace{f_t(E_F - eV + \varepsilon)\,\rho_t(E_F - eV + \varepsilon)}_{\text{occupied tip states}}\underbrace{[1 - f_s(E_F + \varepsilon)]\,\rho_s(E_F + \varepsilon)}_{\text{unoccupied sample states}}\underbrace{|M(E_F - eV + \varepsilon, E_F + \varepsilon)|^2}_{\text{tunneling probability}}d\varepsilon$$

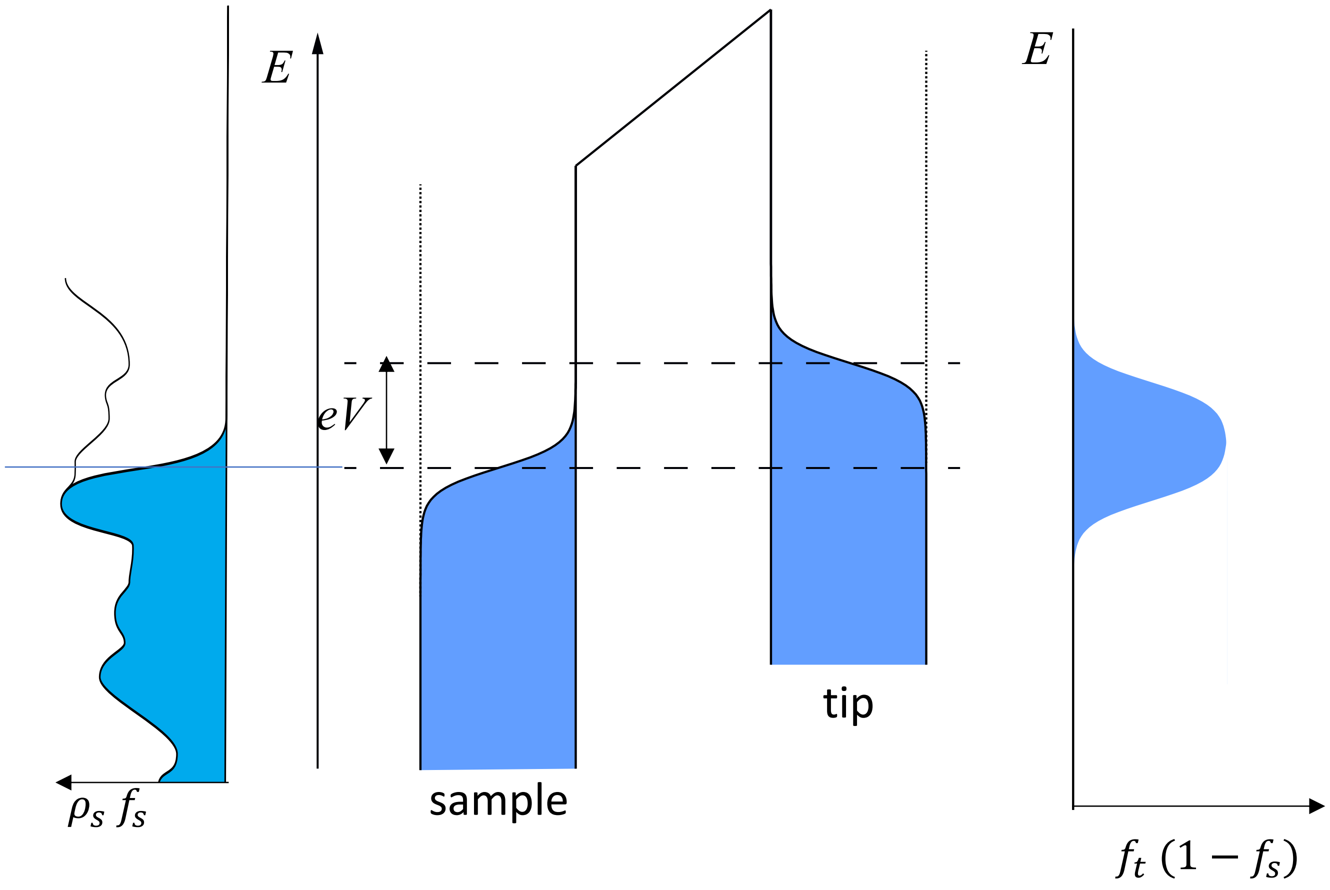

note that the actual DOS of sample (and of tip) are not constant on this energy scale

Tunneling current

$$I = I_{t\to s} - I_{s\to t} = \frac{4\pi e}{\hbar}\int_{-\infty}^{+\infty} [f_t(E_F - eV + \varepsilon) - f_s(E_F + \varepsilon)]\ \rho_t(E_F - eV + \varepsilon)\rho_s(E_F + \varepsilon)|M(\varepsilon)|^2 d\varepsilon$$

For low temperature $(k_B T \ll eV)$ → Fermi function = step function

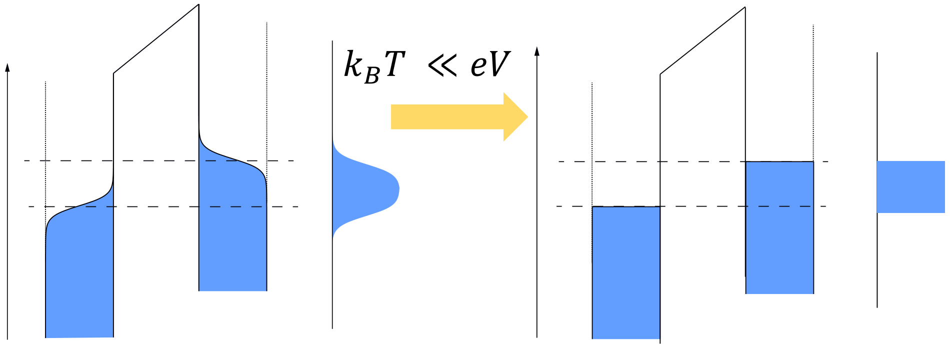

(for $V>0$)

$$I = \frac{4\pi e}{\hbar}\int_{0}^{eV} \rho_t(E_F - eV + \varepsilon)\,\rho_s(E_F + \varepsilon)|M(\varepsilon)|^2 d\varepsilon$$

For very small bias $(eV \ll \Phi)$ → ρ_s , ρ_t constant, values at E_F

$$I = \frac{4\pi e^2}{\hbar} V\, \rho_t(E_F)\, \rho_s(E_F)\, |M|^2$$

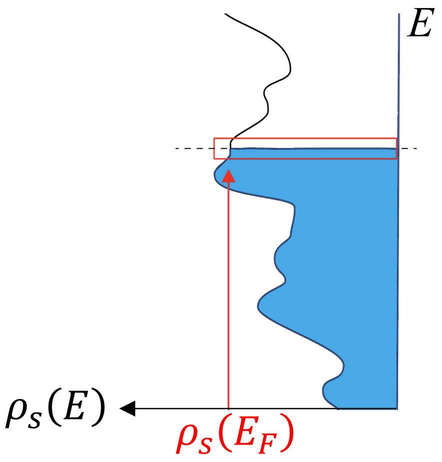

In these hypothesis, the tunneling current is a function of tip and sample density of states close to the Fermi level

STM tunneling current

What about the tunneling matrix $|M|^2$, i.e. the tunneling probability? Its determination requires the knowledge of sample and tip wavefunctions.

For relatively small bias voltages (± 1 V), most of the tunneling current flows between the apex atom and the atom just under it. $|M|^2$ is well described by a simple 1D tunneling probability:

$$|M|^2 = \exp\left[-2d\underbrace{\sqrt{\frac{2m}{\hbar^2}\left(\underbrace{\frac{\Phi_s + \Phi_t}{2} + \frac{eV}{2}}_{e\Phi_{eff}} - \varepsilon\right)}}_{\kappa}\right] = \exp(-2\kappa d)$$

For very small bias: $I \propto V\rho_S(E_F)\rho_T(E_F)e^{-2\kappa d}$

$$\kappa \sim \sqrt{\frac{2m}{\hbar^2}\Phi_{eff}} \sim 0.51\sqrt{\Phi}\ \text{Å}^{-1}$$

$$\boxed{I \propto V\rho_s(E_F)\rho_t(E_F)e^{-1.025\sqrt{\Phi}\,d}}$$

Φ in [eV]; d in [Å]

Typical Φ = 4 - 5 eV

STM vertical resolution

$$I \propto V \rho_s(E_F)\rho_t(E_F)e^{-1.025\sqrt{\Phi}d}$$

Φ in [eV]; d in [Å]

Typical Φ = 4 - 5 eV

Typical set point (actually not really very low bias): V= 1 V; I = 1 nA $\rightarrow d \sim 5$ Å

Atomic step: Δd = 2 Å

$d - \Delta d$: $\quad \dfrac{\Delta I}{I} \approx e^{1.025\sqrt{\Phi}\,\Delta d} - 1 \approx 50$ to 100

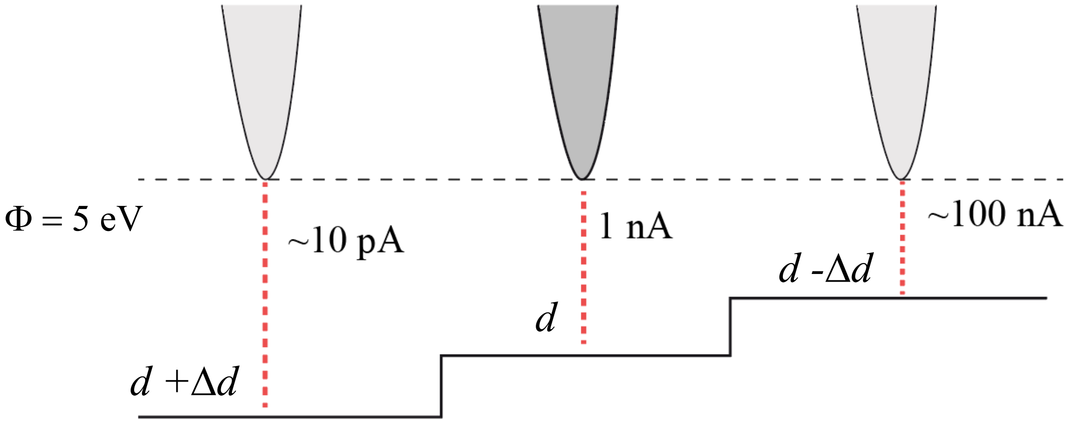

Atomic corrugation: Δd = 0.05 Å

$d - \Delta d$: $\quad \dfrac{\Delta I}{I} \approx e^{1.025\sqrt{\Phi}\,\Delta d} - 1 \approx 0.1$ to 0.2

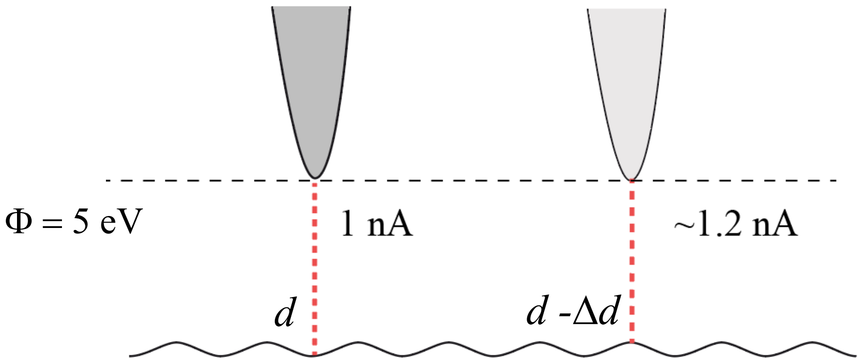

Resolution: Role of atomic states (orbitals) of tip and sample

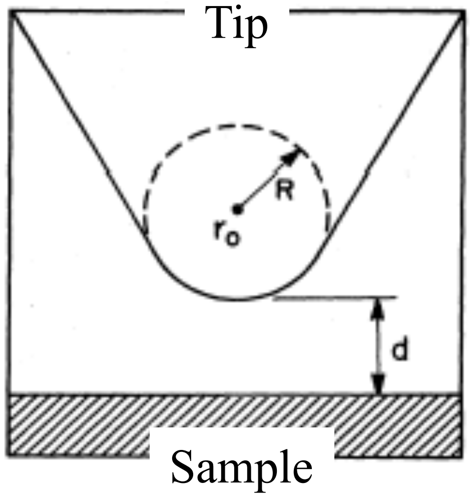

$$I \propto V \rho_S(E_F, r_0)\rho_T(E_F)e^{-1.025\sqrt{\Phi}d}$$

The tunneling current depends on the surface DOS at the tip position, the local DOS (LDOS)

Better evaluation of $|M|^2$ **?**

J. Tersoff and D. R. Hamann, Phys. Rev. B **31**, 805 (1985): s-orbital tip

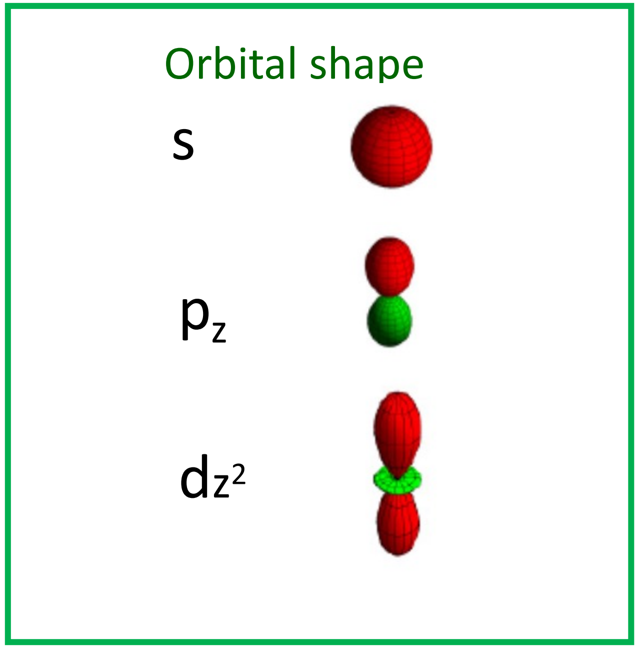

Corrugation dependence on tip and sample electronic state

Tip state	Sample state	Corrugation amplitude $\Delta z(z)$	Ratio
s	s	$[9\kappa/\gamma^2]\ \exp\{-[\gamma-2\kappa]z\}$	1
s	p	$[\gamma/2\kappa]^2[9\kappa/\gamma^2]\ \exp\{-[\gamma-2\kappa]z\}$	2.73
s	d	$\{(3/2)[(\gamma/2\kappa)^2-(1/3)]\}^2[9\kappa/\gamma^2]\ \exp\{-[\gamma-2\kappa]z\}$	12.9
p	s	$[\gamma/2\kappa]^2[9\kappa/\gamma^2]\ \exp\{-[\gamma-2\kappa]z\}$	2.73
p	p	$[\gamma/2\kappa]^4[9\kappa/\gamma^2]\ \exp\{-[\gamma-2\kappa]z\}$	7.45
p	d	$[\gamma/2\kappa]^2\{(3/2)[(\gamma/2\kappa)^2-(1/3)]\}^2[9\kappa/\gamma^2]\ \exp\{-[\gamma-2\kappa]z\}$	35.2
d	s	$\{(3/2)[(\gamma/2\kappa)^2-(1/3)]\}^2[9\kappa/\gamma^2]\ \exp\{-[\gamma-2\kappa]z\}$	12.9
d	p	$[\gamma/2\kappa]^2\{(3/2)[(\gamma/2\kappa)^2-(1/3)]\}^2[9\kappa/\gamma^2]\ \exp\{-[\gamma-2\kappa]z\}$	35.2
d	d	$\{(3/2)[(\gamma/2\kappa)^2-(1/3)]\}^4[9\kappa/\gamma^2]\ \exp\{-[\gamma-2\kappa]z\}$	166

Materials with highly directional electronic orbitals give better resolution

TABLE I. Fermi-level DOS of common tip materials (Ref. 13).

Material	W	Pt	Ir
s state	3.1%	0.77%	0.94%
d state	85%	98%	96%

C. J. Chen. *Phys. Rev. B*. **42**, 8841 (1990);
C. J. Chen. *J. Vac. Sci. Technol. A* **9**, 44 (1991).

Tip preparation

Tungsten wire

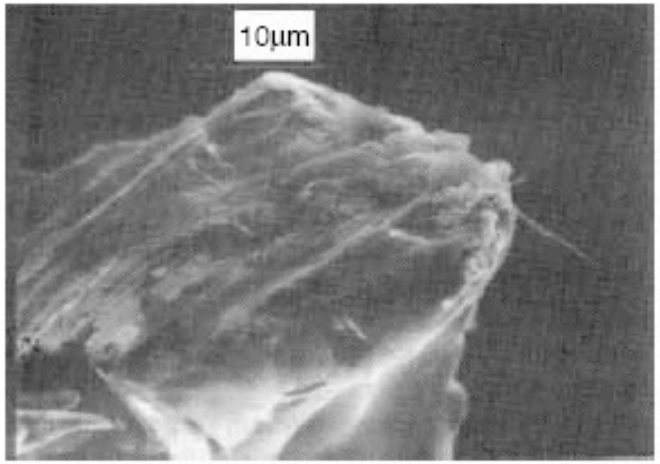

After electro-erosion (etching)

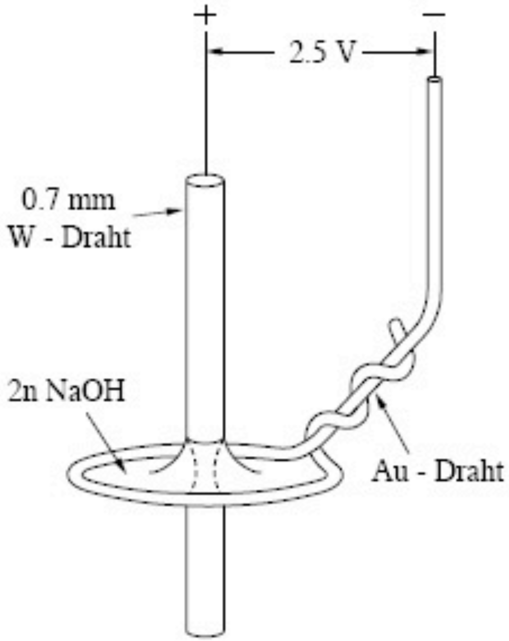

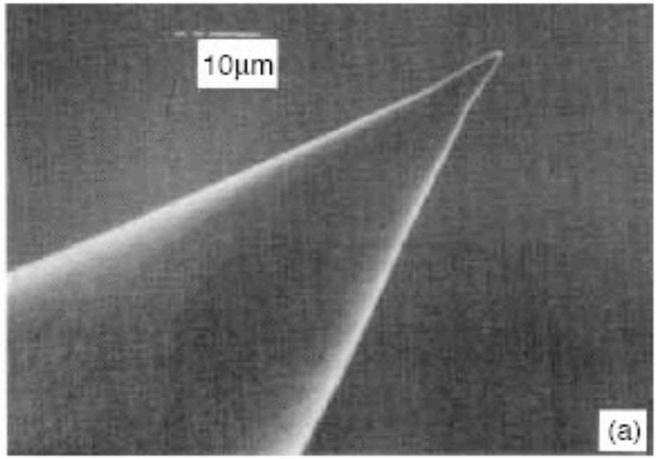

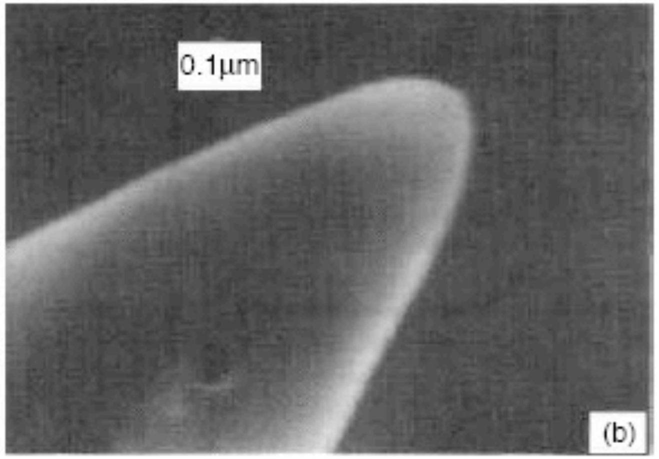

Tip preparation

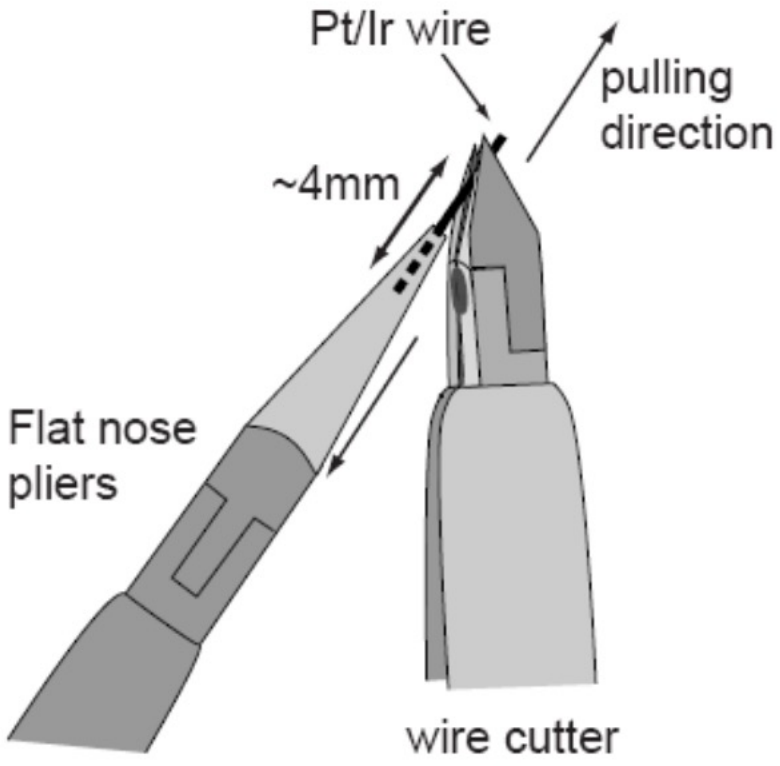

$Pt_{90}Ir_{10}$
$Pt_{80}Ir_{20}$

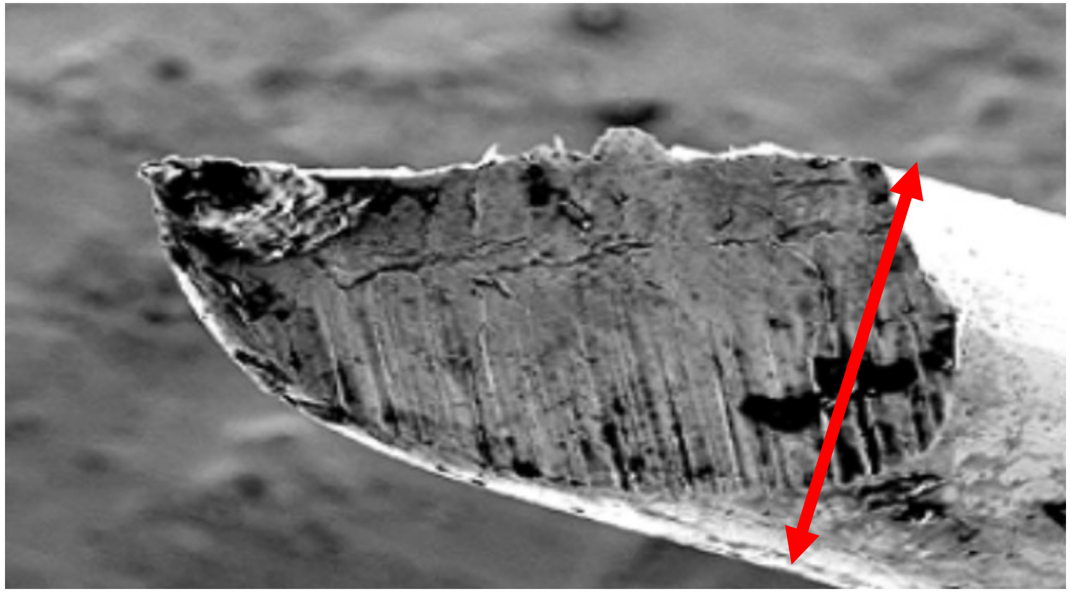

0.2 mm

STM design: Beetle type

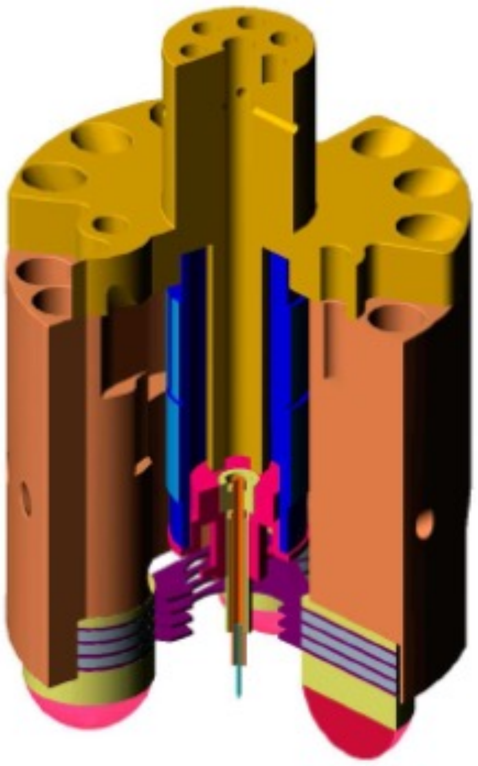

Vue en coupe

1 cm

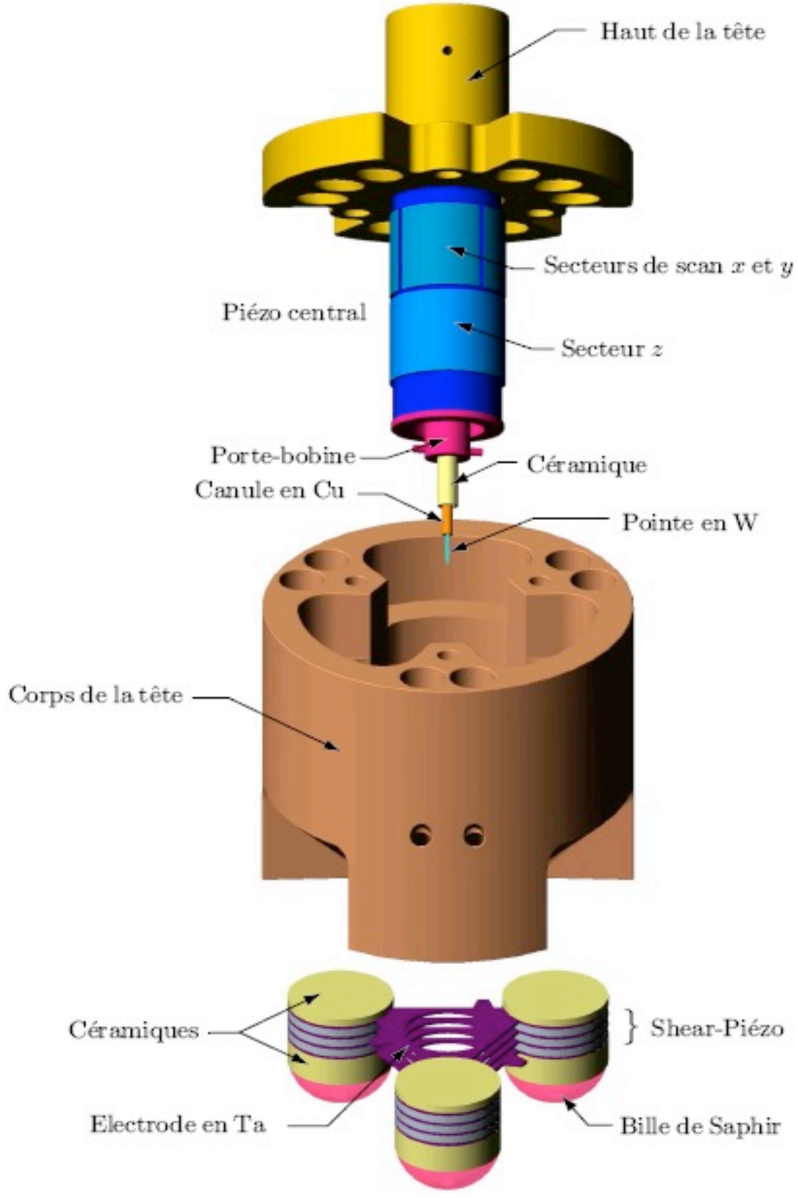

Vue éclatée

N. Weiss, EPFL PhD thesis

Variable Temperature UHV-STM

Beetle-STM Principle

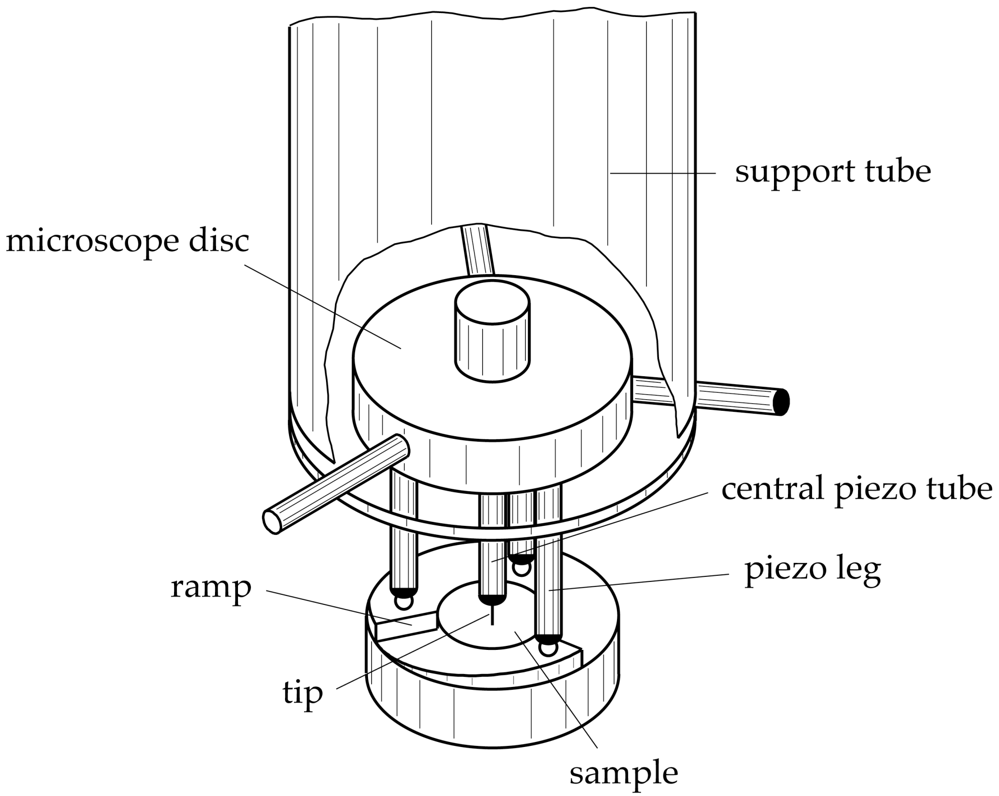

J. Frohn, J. F. Wolf, K. Besocke, M. Teske, Rev. Sci. Instrum. **60**, 1200 (1989)

STM design: IBM-Unil

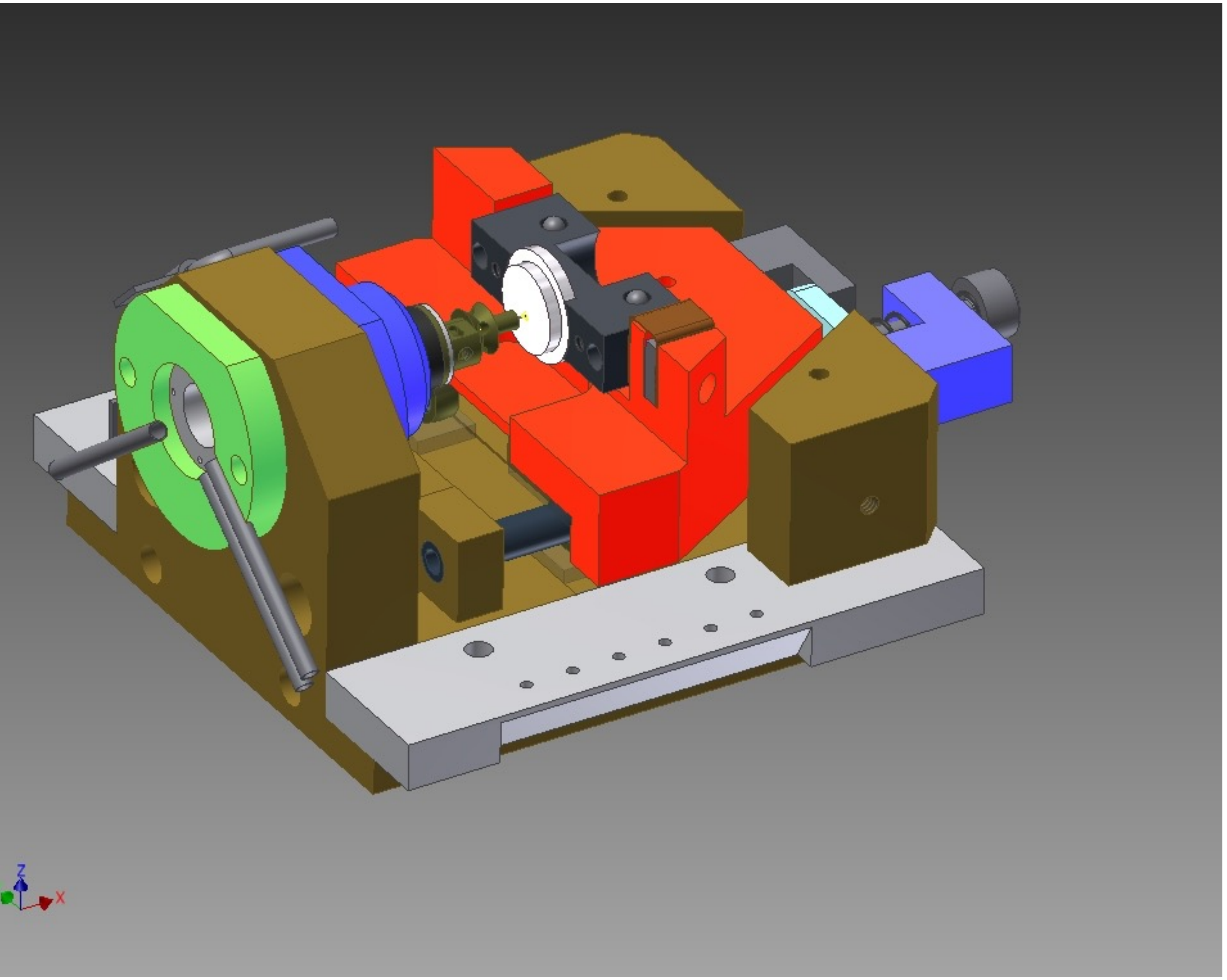

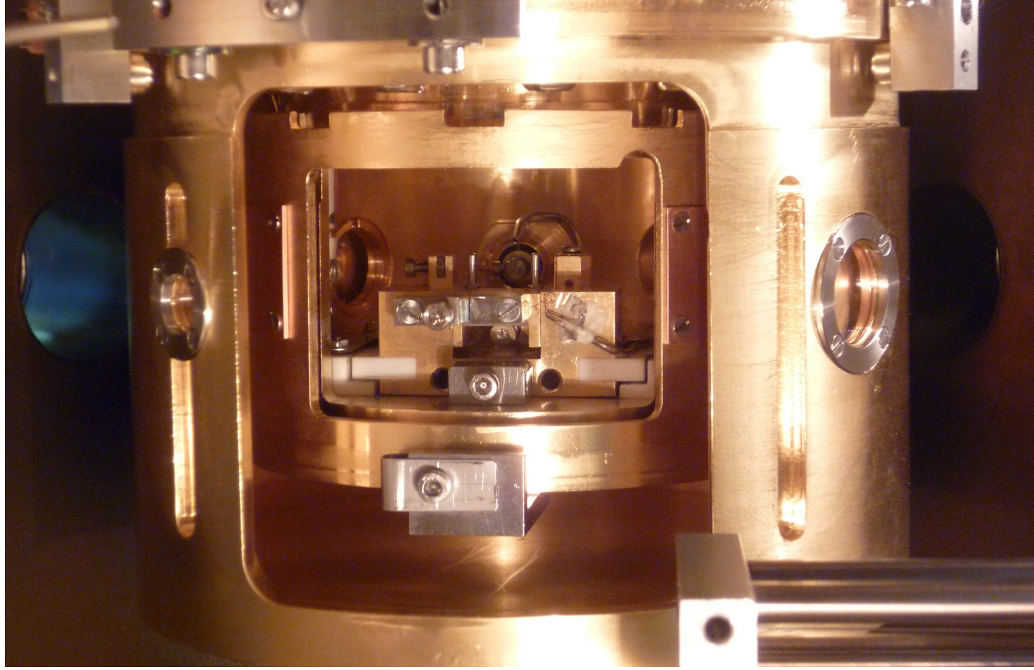

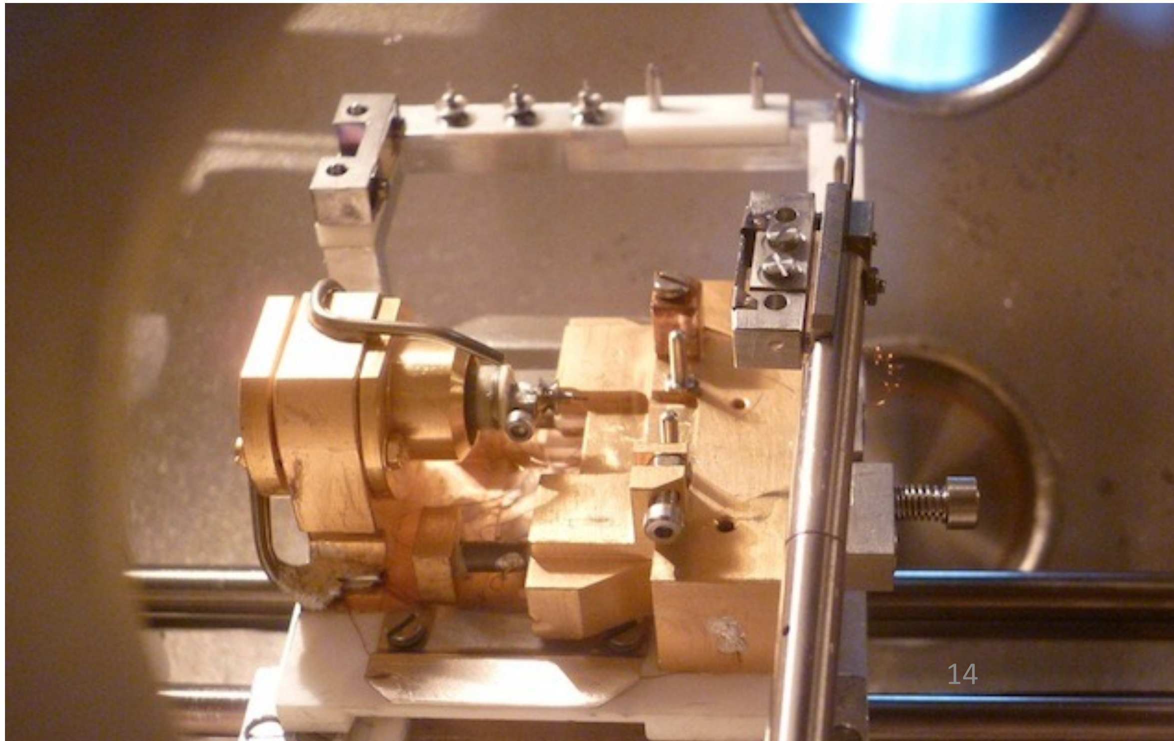

R. Gaisch, Unil PhD Thesis

Not for free…

1 M€

100 K€

10 K€

Table-top STM

VT UHV STM

UHV ^{3}He cryo-STM

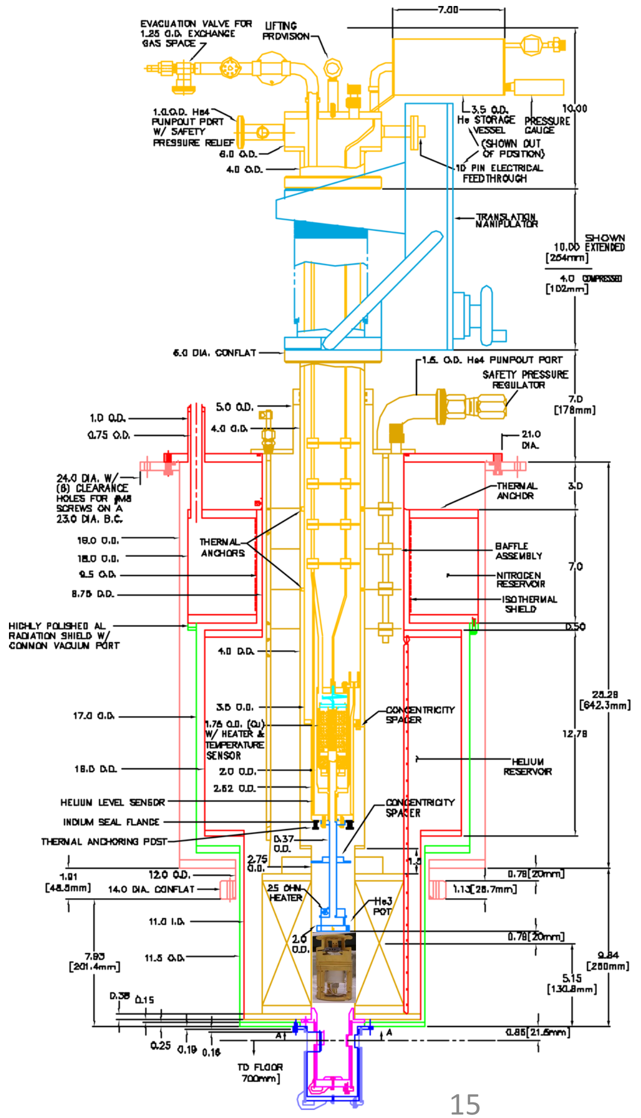

Imaging and topography

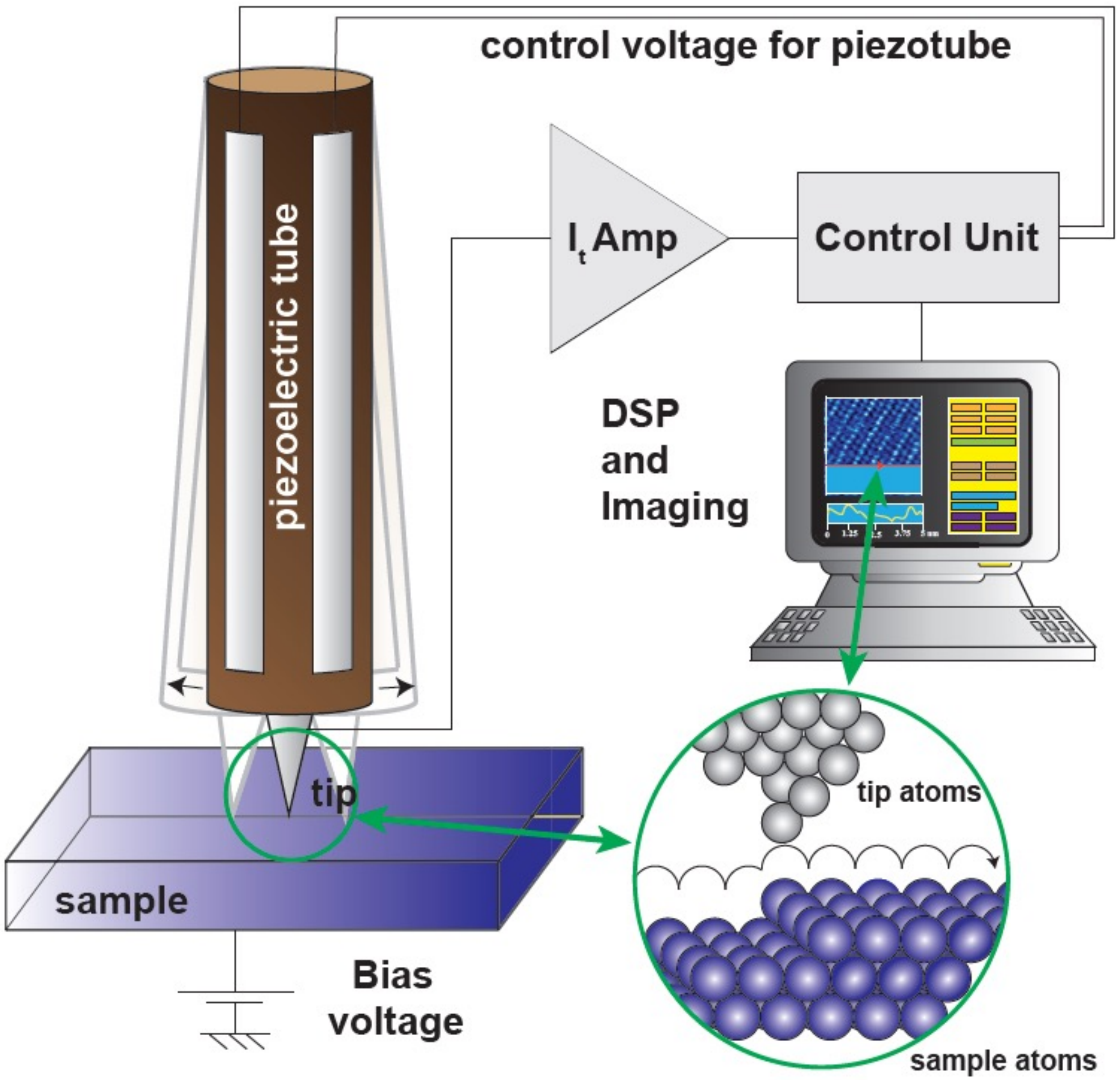

STM imaging modes

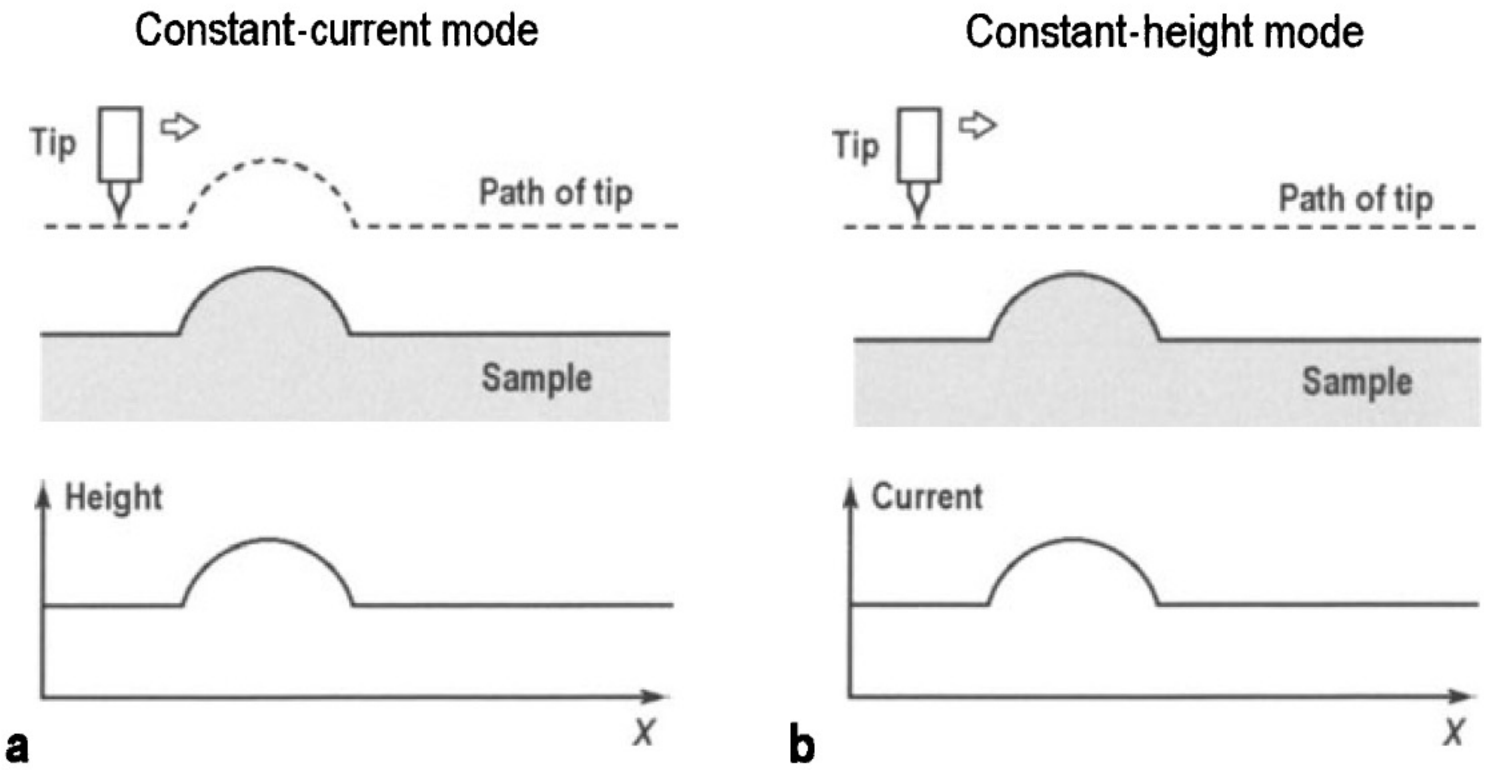

Imaging and topography

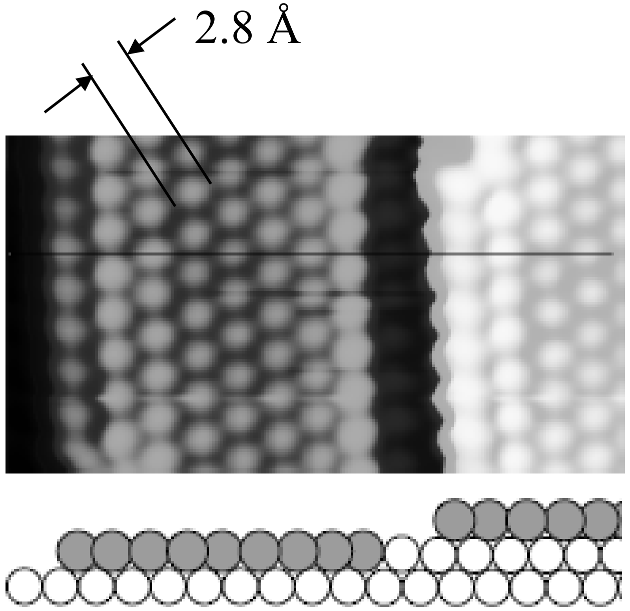

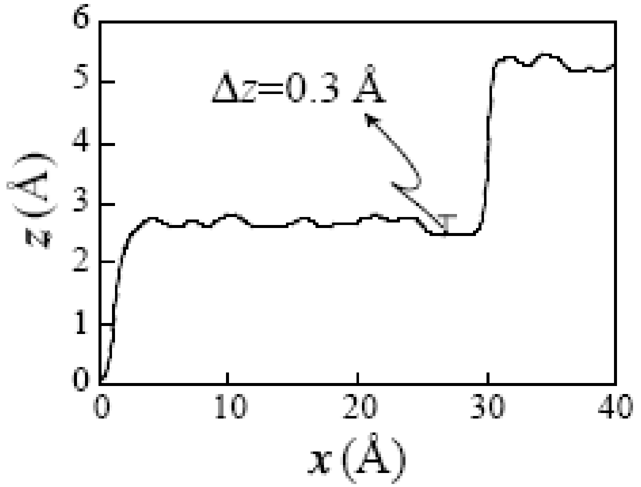

Constant current image of a stepped Pt surface covered by 1 monolayer Ag (I = 2.7 nA, V = 10 mV)

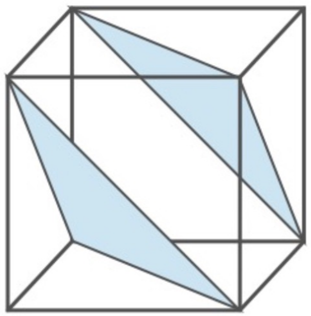

111 planes (Pt fcc, a = 3.9 Å)

P. Gambardella,
EPFL PhD thesis

<u>fcc- and hcp- hollow sites on Al(111)</u>

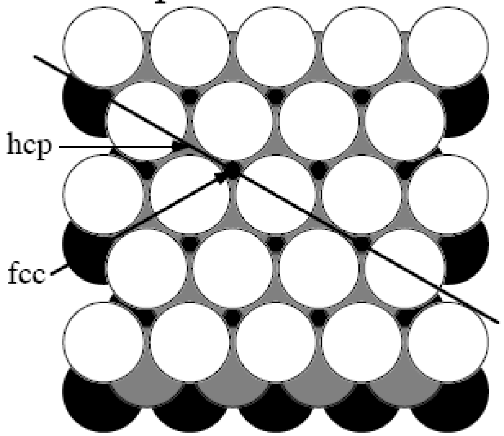

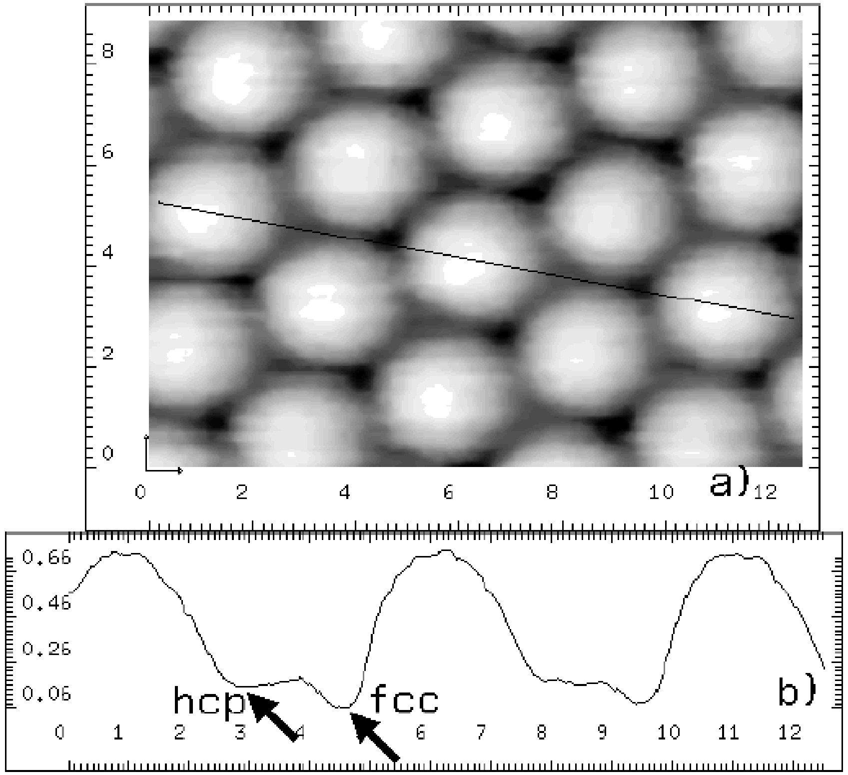

H. Brune PhD thesis

Warning !!!!

$$\boxed{I \propto V\rho_S(E_F)\rho_T(E_F)e^{-1.025\sqrt{\Phi}d}}$$

Remember: the tunneling current is a measure of the Local Density of States of tip and sample (for very low bias is the LDOS at the Fermi level)

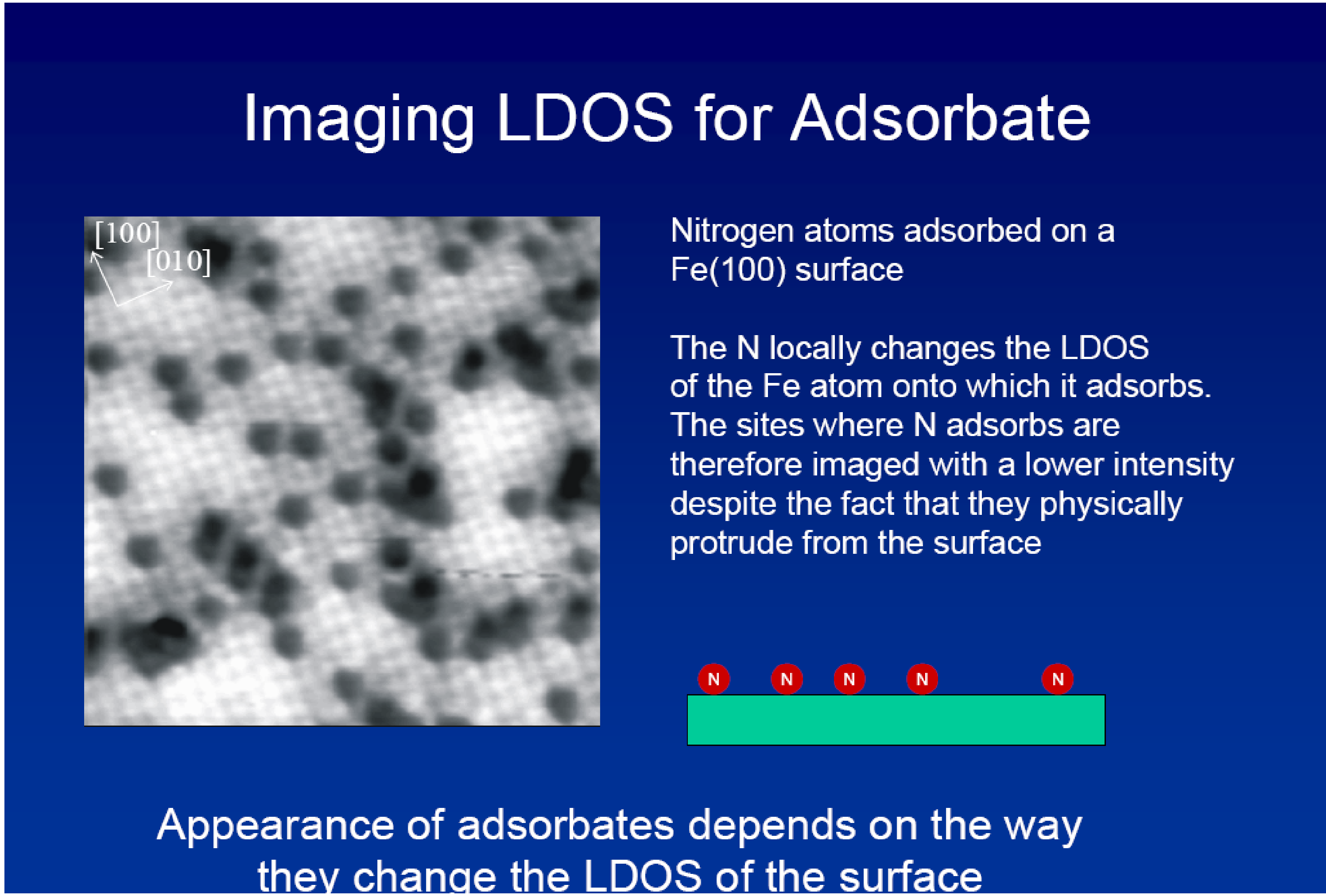

AFM: Atomic Force Microscope

AFM enables atomic-scale imaging of insulating surfaces.
The tip is mounted on a cantilever and is brought into contact with the sample surface. The force on the cantilever is related to its deflection via Hooke's law: $F = -kx$, where k is the spring constant of the cantilever and x is the deflection.

Lennard-Jones
type potential:
sum of two terms

repulsive (Pauli), dominates at very short distance
+
attractive (van de Waals), dominates at larger distance
→
minimum

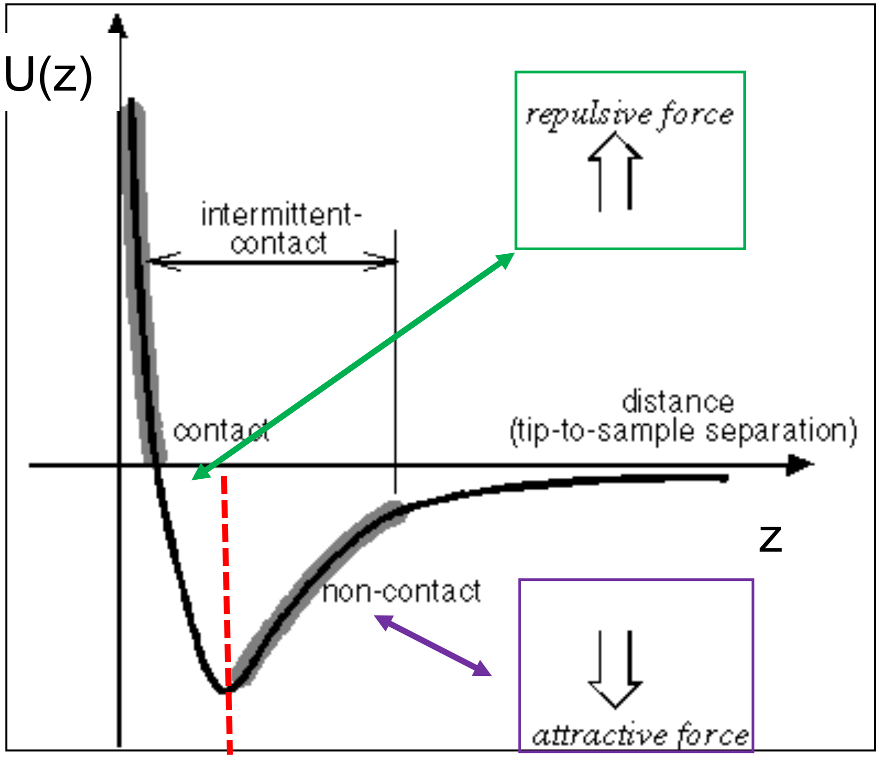

2-3 Å

Potential $U(z)$ seen by the tip apex approaching a surface

$$F = - dU/dz$$

Optical detection of the cantilever deflection

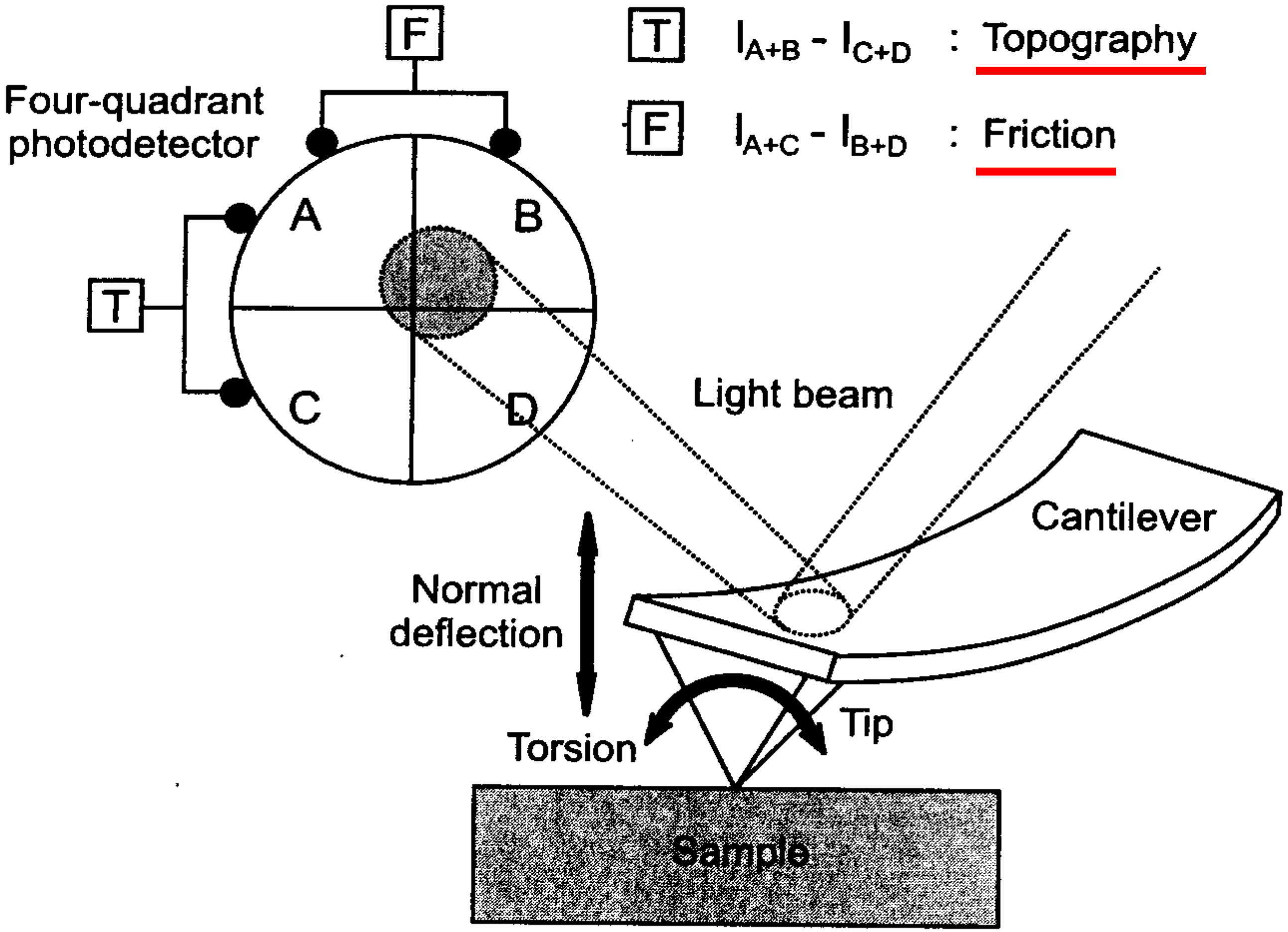

The attractive or repulsive force between the tip and the sample causes a deflection of the cantilever towards or away from the sample.
The deflection is measured by a laser beam directed at the back of the cantilever. As the cantilever deflects, the angle of the reflected beam changes, and the spot falls on a different part of the photodetector.
The signals from the four quadrants of the detector are compared to calculate the deflection signal.

AFM cantilever

SEM images

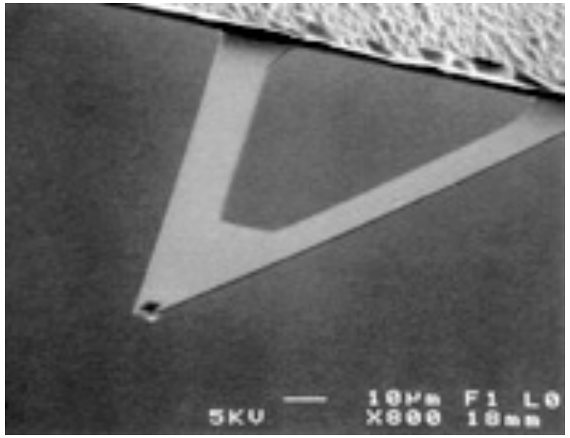

Sketch

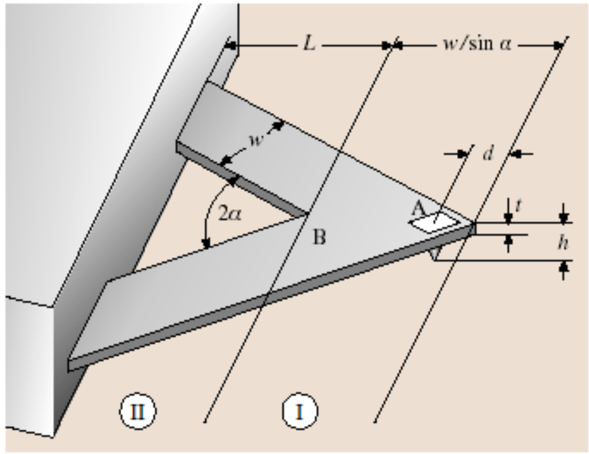

Zoom on the tip

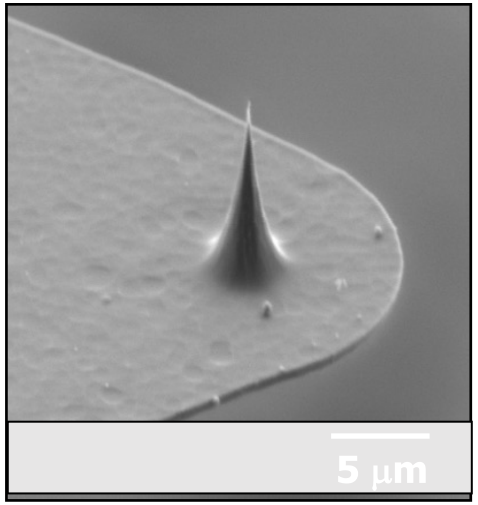

Contact mode

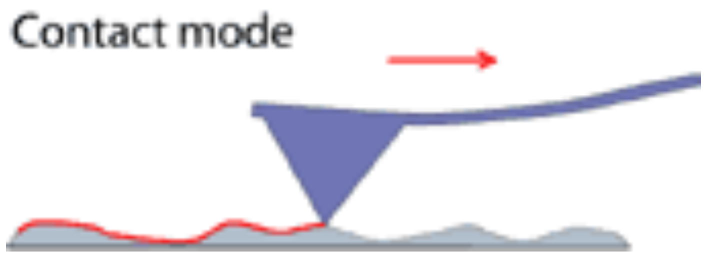

Contact mode:
- tip-surface distance < 2-3 Å

$F(x) = -k\,x$ Hooke's Law

If the spring constant of the cantilever is smaller than the surface one, then the cantilever bends.
If the spring constant of the cantilever is larger than the surface one, then the surface is deformed.
This mode can be used for very high resolution imaging, such as atomic resolution, but not on "soft" surface that could get deformed

Non-contact mode

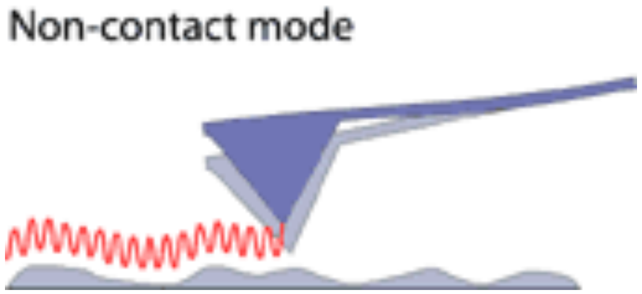

Non-contact mode:
- tip-surface distance ~ 5 Å
- Less destructive (for soft or elastic surfaces)

The cantilever holding the tip is vibrating at its resonant frequency (ω_0) using a piezoelectric element while far from the surface (assuming no interaction). As the tip is moved towards the surface, the presence of a force gradient modifies the spring constant of the cantilever so that $k_{eff} = k - F'$ where k is the spring constant of the cantilever in the absence of a tip-sample interaction and $F'=F_{ts}$ is the tip-sample interaction. This modification of the spring constant will produce a shift of the resonant frequency of the cantilever given by:

$$\omega = \sqrt{\frac{k_{eff}}{m}} = \sqrt{\frac{k - F'}{m}}$$

$$= \left(\sqrt{\frac{k}{m}}\right)\sqrt{1 - \frac{F'}{k}}$$

$$= \omega_0 \sqrt{1 - \frac{F'}{k}}$$

Contact *vs* non-contact mode

Polymer on a surface

contact non-contact

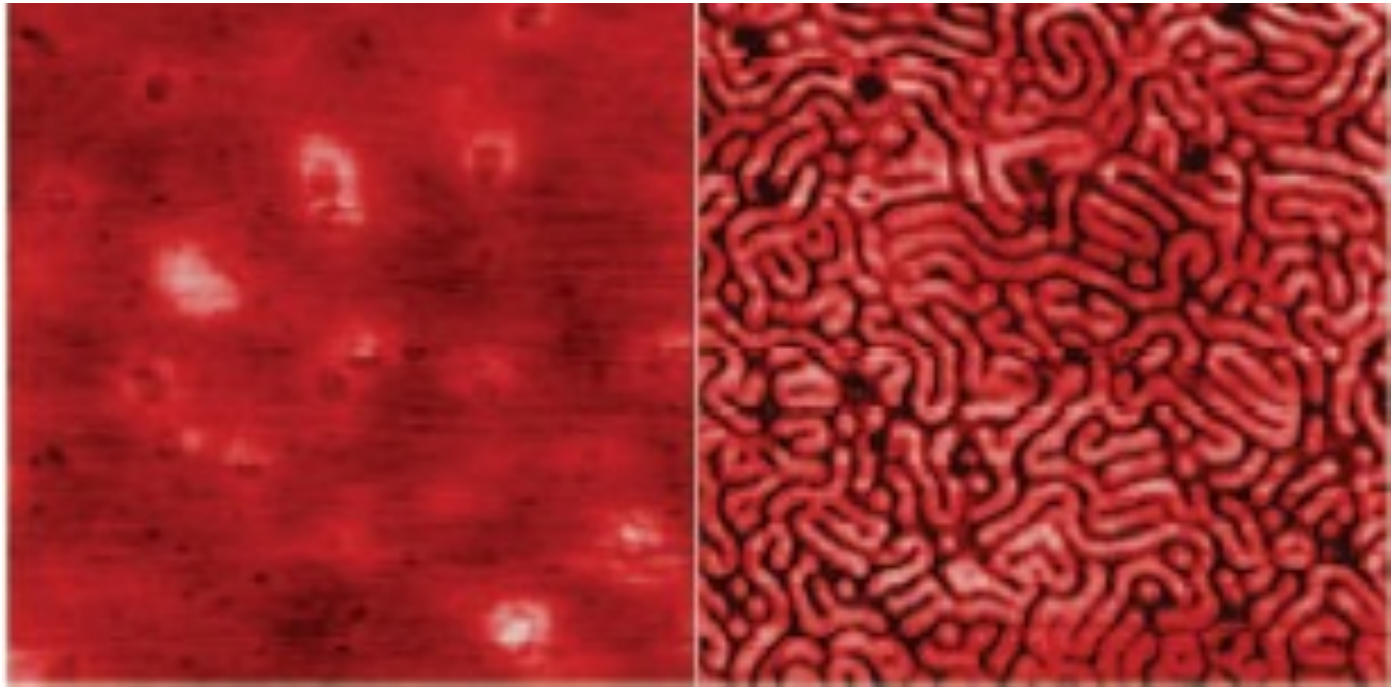

Chemical identification of individual surface atoms by AFM

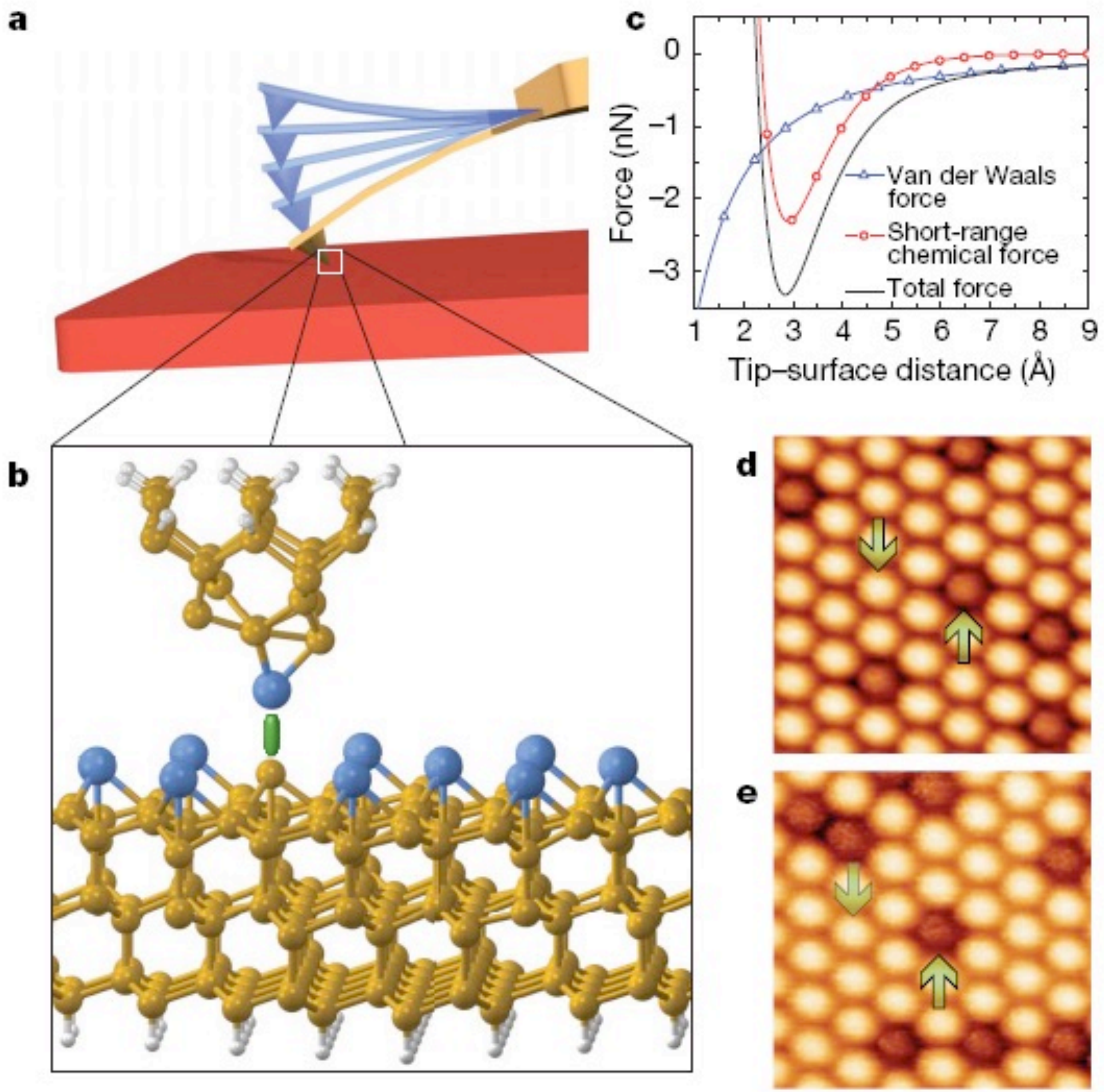

(a) Schematic illustration of AFM operation in dynamic mode
(b) Onset of the chemical bonding between the outermost tip atom and a surface atom that gives rise to the atomic contrast (short green line)
(c) However, the tip experiences not only the short-range force associated with this chemical interaction, but also long-range force contributions that arise from van der Waals and electrostatic interactions between tip and surface. Curves obtained with analytical expressions for the van der Waals force, the short-range chemical interaction force, and the total force to illustrate their dependence on the absolute tip–surface distance.
(d) Dynamic force microscopy topographic images of a single-atomic layer of Sn (d) and Pb (e) grown, respectively, over a Si(111) substrate. At these surfaces, a small concentration of substitutional Si defects, characterized by a diminished topographic contrast, is usually found. Image dimensions are (4.3x4.3)nm^2

B 5	C 6	N 7	O 8	F 9	Ne 10
Al 13	Si 14	P 15	S 16	Cl 17	Ar 18
Ga 31	Ge 32	As 33	Se 34	Br 35	Kr 36
In 49	Sn 50	Sb 51	Te 52	I 53	Xe 54
Tl 81	Pb 82	Bi 83	Po 84	At 85	Rn 86

Y. Sugimoto *et al.*, Nature **446**, 64 (2007)

Tuning fork AFM / STM

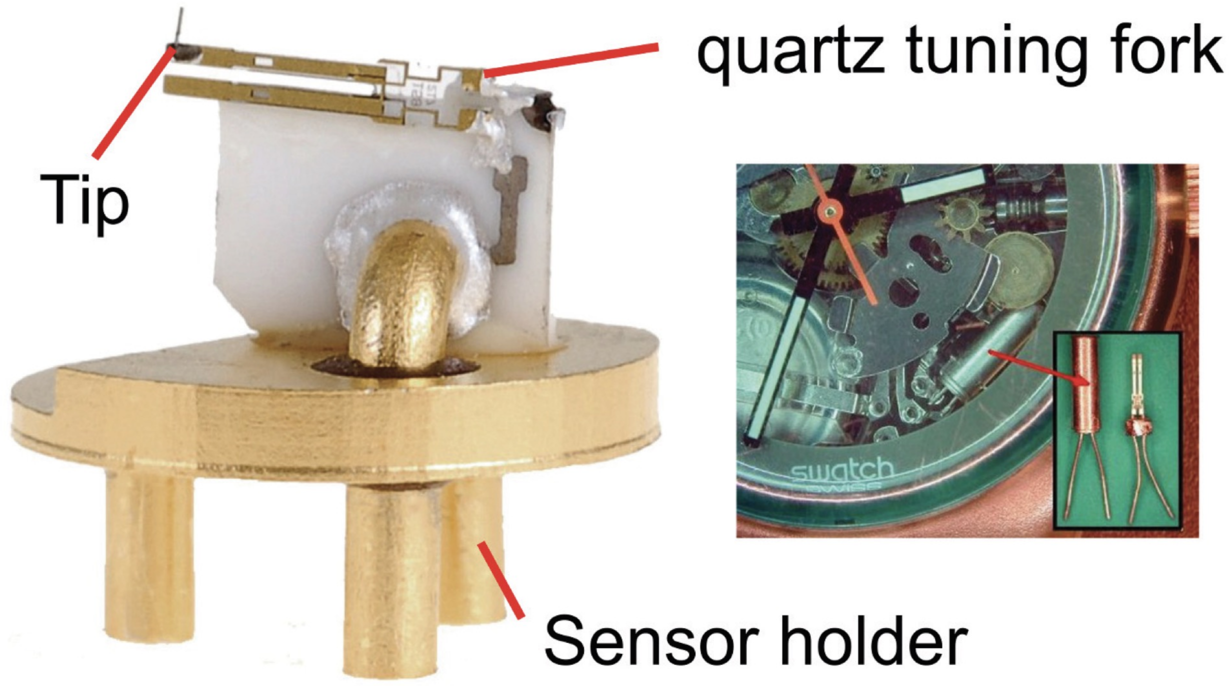

The tip-sample interaction force is
transduced to electric signals
through the piezoelectric effect of quartz

Rev. Sci. Instr. **90**, 011101 (2019)